The Immunoregulatory Effect of Mechanical Stress on Three-dimensional Cultured Mesenchymal Stem Cells After Extensive Expansion

Fang-Ying Du
Xi'an Jiaotong University
Na Zhao
Xi'an Jiaotong University Second Affiliated Hospital
Lei Bao
Xi'an No.4 Hospital
Jing Lei
Xi'an No.4 Hospital
An-Qi Liu
Xi'an Institute of Tissue Engineering and Regenerative Medicine
Ying-Feng Gao
Xi'an Institute of Tissue Engineering and Regenerative Medicine
Li-Hui Bao
Xi'an Institute of Tissue Engineering and Regenerative Medicine
Hua Ni
Xi'an Institute of Tissue Engineering and Regenerative Medicine
Feng Zhou
Xi'an No.4 Hospital
Xiao-Rui Yu
Xi'an Jiaotong University
Cheng-Hu Hu (chenghu@xiterm.com)
Xi'an Jiaotong University Second Affiliated Hospital https://orcid.org/0000-0003-2443-6485

Research

Keywords: Extensive expansion, Immunomodulatory, Mechanical stress, Mesenchymal stem cells, Three-dimensional culture

Posted Date: September 20th, 2021

DOI: https://doi.org/10.21203/rs.3.rs-889481/v1

Abstract

Background: Mesenchymal stem cells (MSCs) have been used to treat immunopathy, and three-dimensional (3D) cultured MSCs show enhanced immunomodulatory property compared with those in two-dimensional (2D) culture. However, both the regulatory mechanisms remain unclear. The aim of the study was to investigate the role of mechanical stress in maintaining the immunomodulatory function of 2D and 3D cultured MSCs.

Methods: Umbilical cord mesenchymal stem cells (UC-MSCs) were plated on tissue culture plastic (TCP) as 2D culture and 3D cultured UC-MSCs were seeded in matrigel. Surface markers, clonogenicity, proliferation and immunoregulatory property of UC-MSCs were evaluated. Meanwhile, we established the mouse models of colitis and type 1 diabetes mellitus (T1DM) to reveal the pharmacotherapeutic effects of 3D cultured MSCs in vivo. The effect of changing mechanical stress by modulating Yes-associated protein (YAP) on immunomodulatory function of 2D and 3D cultured UC-MSCs was evaluated by immunofluorescent analysis, real-time quantitative polymerase chain reaction (qPCR) and western blot.

Results: We verified early passage UC-MSCs in 2D and 3D cultures exhibited stemness, immunomodulatory property and therapeutic efficacy against immunopathy. However, these characteristics of 2D cultured UC-MSCs were impaired after extensive expansion, whereas 3D culture extended them for several passages by activating YAP. Moreover, prostaglandin E2 (PGE2) could up-regulate YAP to improve the immunomodulatory ability of 2D cultured UC-MSCs after extensive expansion.

Conclusions: This work found for the first time that the significance of mechanical stress in maintaining immunoregulatory function of 2D and 3D cultured UC-MSCs, providing a new idea for improving the efficacy of MSCs-based immunotherapy.

1. Background

Mesenchymal stem cells (MSCs) are a subset of multipotent stem cells with the capacity of immunomodulation, which makes them promising candidates for stem-cell-based therapies [1]. Noteworthy is that although cell replacement plays an important role in the treatment of MSCs, the ultimate therapeutic effects are mainly the results of the immunomodulatory ability of MSCs, which reacts with the immune system [2, 3]. It is well recognized that MSCs exert significant protective effects against immunopathy type 1 diabetes mellitus (T1DM) by inhibiting the expression of cytokines, such as interleukin (IL)-6, IL-1β, tumor necrosis factor (TNF)-α and IL-10, and the therapeutic effects persist during the long follow-up period [4, 5]. Furthermore, MSCs can also modulate regulatory T (Treg)/ T helper (Th)17 cells in the spleen and improve endoscopic findings, pathological findings, Mayo scores and inflammatory bowel disease quality scores in colitis [6, 7]. However, the mechanism by which MSCs treat immunopathy remains unclear, and discussing such content will help to further improve the therapeutic effects of MSCs on immunopathy.

Increasing evidences have indicated that MSCs cultured in 2D and 3D systems exhibited significant differences in cell morphology, proliferation, differentiation abilities and energy metabolism [8]. Under 2D culture conditions, replicative senescence can be induced by cell extensive expansion, which limit the efficacy of transplanted MSCs [9–12]. 3D culture is developed on the basis of 2D monolayer, but with the characteristics of microenvironments in vivo [13, 14]. Thus, 3D cultured MSCs have been shown to enhance many therapeutic properties, including their immunosuppression and immunoregulation [1, 15, 16]. One study found several genes closely related to immune regulation, such as human leukocyte antigen (HLA)-G, indoleamine 2,3-dioxygenase (IDO)-1, prostaglandin synthase (PTGS)-2 and transforming growth factor (TGF)-β1 were more highly expressed after 3D culture than that after 2D culture. Further, 3D cultured MSCs could inhibit the proliferation of activated lymphocytes more effectively [17]. However, the mechanism of maintaining cellular immunomodulatory ability in 3D culture has not been reported, and exploring this mechanism provides an experimental basis for further elucidating the immunomodulatory characteristic of MSCs in 3D culture.

It has been known that Yes-associated protein (YAP) signaling is strongly activated during the culture of cells in a matrigel-encapsulated 3D culture system and maintains the proliferative capacity of the encapsulated cells [18]. Recent studies have shown that variation in the stiffness of 3D matrix changed mechanical stress, and was a potent regulator of MSCs expansion and differentiation. This may be due to the fact that YAP serves as a downstream nuclear mediator and effector of actin cytoskeletal contraction through β-catenin [19–21]. However, it is unknown whether activated YAP can improve the immunomodulatory ability of MSCs, the research in this regard may helpful to reveal the mechanism by which MSCs participate in immunoregulation through YAP in 3D culture, and to provide a research basis for exploring the way to enhance the immunomodulatory function of MSCs.

In the present study, we firstly verified that compared with 2D culture, 3D culture did extend the stemness and immunosuppression of UC-MSCs for several passages, as well as employed immune disorders such as colitis and T1DM mouse models to confirm the therapeutic effects of long-term passaged UC-MSCs in 3D culture. Furthermore, we explored the modulation of YAP pathway both in 2D and 3D cultured UC-MSCs and its therapeutic effects in colitis and T1DM mouse models, so as to prove the significance of mechanical stress in maintaining immunoregulatory function of 2D and 3D cultured UC-MSCs, and prostaglandin E2 (PGE2) could be used to up-regulate YAP and improve the immunomodulatory ability of 2D cultured UC-MSCs after extensive expansion. To the best of our knowledge, it was found for the first time that the mechanical stress played a significant role in maintaining the immunomodulatory function and therapeutic potential both of 2D and 3D cultured UC-MSCs.

2. Methods

2.1 Animals

Four-week-old male C57BL/6J mice were purchased from the Laboratory Animal Center of the Fourth Military Medical University. The mice were housed with a 12 h/12 h light/dark cycle at an ambient

temperature of 22–25℃ with free access to food and water. All animal experimental procedures were accordance with National Institutes of Health Guide for the Care and Use of Laboratory Animals and approved by Animal Care Committee of Xi'an Jiaotong University.

2.2 Isolation and Culture of UC-MSCs

UC-MSCs were isolated from human umbilical cords freshly obtained from women who gave birth in Xi'an No. 4 Hospital. All the donors signed informed consent to this study. The experimental procedures of human samples were approved by the Institutional Review Board for Human Subjects Research of Xi'an No. 4 Hospital. The umbilical cord was careful removal of blood vessels, Wharton's jelly tissue was chopped into small pieces of 1 mm^3 and seeded in minimum essential medium-α (α-MEM, Gibco, USA, 12000063) with 10% fetal bovine serum (FBS, Gibco, USA, 16140071), as described in previous reports [22]. 5–7 days after seeding, the cells reached 80% confluency, then passaged and cultured in α-MEM supplemented with 10% FBS, streptomycin (100 IU/ml, Gibco, USA, 15140122) and penicillin (100 μg/ml, Gibco, USA, 15140122), and maintained in a humidified 5% CO_2 incubator at 37℃.

In the 2D method, UC-MSCs at P3 were plated directly on tissue culture plastic (TCP) and passaged using 2.5% trypsin (Gibco, USA, 15050057). In the 3D method, UC-MSCs at P3 were seeded in matrigel (Corning, USA, 356231) and passaged with cell recovery solution (Corning, USA, 354253). MSCs were continuously passaged until P15. Cells at P5 and P15 were used in the following studies.

2.3 Flow Cytometry Analysis of Cell Surface Markers

Cell phenotypes of P5 and P15 of both 2D and 3D cultured UC-MSCs were detected by flow-cytometric analysis to measure the expression of stem cell surface markers. Approximately 5×10^5 UC-MSCs were harvested. Then, the single-cell suspension was re-suspended and incubated with the following fluorescent antibodies: CD73 (BD Bioscience, 561254), CD105 (BD Bioscience, 560839), CD90 (BD Bioscience, 561970), HLA-Ⅱ(BD Bioscience, 555561), CD34 (BD Bioscience, 550761) and CD45 (BD Bioscience, 555485). The samples were measured by flow cytometric analysis using a Beckman Coulter Epics XL cytometer (Beckman Coulter, USA).

2.4 Fibroblastic Colony-forming Assay

2D or 3D cultured UC-MSCs (P5 and P15) were harvested and 3×10^2 cells were seeded on 6-well cell culture cluster containing α-MEM medium. The medium was refreshed every 3 days. After culturing for 10 days, the plates were rinsed with phosphate buffer saline (PBS, Sigma-Aldrich, USA, P5493) and the cells were fixed by 4% paraformaldehyde (Sigma-Aldrich, USA, 158127). The colonies were stained by 1% (w/v) toluidine blue solution (Sigma-Aldrich, USA, 89640).

2.5 Cell Proliferation Assay

P5 and P15 UC-MSCs (5×10^2 cells/well) were seeded on 96-well plates. Cell proliferation was analyzed with cell counting kit-8 (CCK-8, Yeasen Biotech, China, 40203ES60) according to the standard protocol. First, 10 μL CCK-8 solution per 100 μL complete medium was added into intraday wells, and the plates

were incubated in 37℃ and 5% CO_2 for 3h after being blended. The optical density (OD) value was recorded by a microplate reader (Bio-TEK Instruments, USA) at 450 nm.

2.6 Isolation of Human Peripheral Blood Mononuclear Cells (PBMCs) and $CD3^+$ T Cells

PBMCs were isolated from fresh whole blood from Xi'an No. 4 Hospital. PBMCs were prepared from peripheral blood diluted in PBS, slowly added to Lymphoprep (MP biomedicals, USA, 0916922-CF), and then centrifuged. The separated PBMCs were collected and washed twice with PBS. $CD3^+$ T cells were then isolated from PBMCs using anti-human CD3 antibody (Biolegend, USA, 300308) and FACS cell sorting system (Miltenyi Biotec, Germany).

2.7 Co-culture of $CD3^+$ T Cells with UC-MSCs

$CD3^+$ T cells (5×10^5 cells/ml) were plated in RPMI 1640 complete medium and stimulated by adding 2 μg/ml CD3 (Novoprotein, China, CMP-A018) and 2 μg/ml CD28 (Novoprotein, China, CMP-A013). The stimulated cells (activated T cells) were co-cultured with the 2D or 3D UC-MSCs (P5 and P15) in the proportion of 1:10 for 3 days. The percentage of $CD4^+IFN\text{-}\gamma^+$-Th1, $CD4^+IL\text{-}4^+$-Th2, $CD4^+IL\text{-}17^+$-Th17 and $CD4^+CD25^+Foxp3^+$-Tregs and the proliferation inhibition were measured. The fluorescent antibodies involved in this study include $CD4^+$ (Biolegend, USA, 357404), $IFN\text{-}\gamma^+$ (Thermo Fisher Scientific, USA, 45-7319-41), $IL\text{-}4^+$ (Thermo Fisher Scientific, USA, 17-7049-41), $IL\text{-}17^+$ (Biolegend, USA, 512303) and $Foxp3^+$ (Thermo Fisher Scientific, USA, 88-8999-40).

2.8 ELISA for Cytokine Production

The supernatant of co-cultured MSCs and activated T cells were collected. Cytokine measurements were done for IL-6 (EHC007), IL-10 (EHC009) and TGF-β (EHC107b), using a commercially available enzyme-linked immunosorbent assay (ELISA, Neobioscience, China) according to the manufacturer's protocol. The serum of experimental T1DM mice was collected. Cytokine measurements were done for Glycated hemoglobin (GHb) and C-peptide (Fankewei, China, F2159-A, F2580-A) by ELISA kit.

2.9 Western Blot Analysis

After collection, protein concentration measurements were carried out using a bicinchoninic acid (BCA) kit (Beyotime Biotechnology, China, P0012). Equal protein amount from each sample was taken for western blot analysis. The protein bands were visualized and captured using Amersham Imager 600 (GE Healthcare Life Sciences, China). Anti-YAP1 antibody (ab56701) was obtained from Abcam (USA). GAPDH antibody (CW0100) was purchased from CWBio (China).

2.10 Immunofluorescent Analyses.

The cells (P5 and P15) were determined at day 3 after seeding by immunofluorescent staining against β-Tubulin antibody (CWBio, China, CW0098) or Anti-YAP1 antibody (Abcam, USA, ab56701). After

incubation with Alexa Fluor 488 and Alexa Fluor 594 conjugated secondary antibodies, 4',6-diamidino-2-phenylindole (DAPI) was used to stain the nuclei.

2.11 RNA Extraction and Real-time Quantitative Polymerase Chain Reaction (qPCR)

RNA was isolated from UC-MSCs using the TRIzol Reagent (Invitrogen,USA, 15596026). The cDNA was transcribed using a PrimeScript RT reagent kit (TaKaRa, Japan, RR036A) and random primers following the manufacturer's instructions. The qPCR analysis was performed using the TB Green Premix Ex Taq II kit (TaKaRa, Japan, RR820L) and detected by CFX96™ Real-time RT-PCR System (Bio-Rad, USA).

2.12 Experimental Colitis and Treatment by UC-MSCs

Colitis was induced in C57/BL6J mice (8 weeks old female) by administration of 2.5% dextran sulfate sodium salt (DSS, MP Biomedicals, USA, 02160110-CF) in drinking water for 5 days followed by normal water. These mice were randomly and evenly divided into 6 groups: normal, DSS + PBS, DSS + P5 2D UC-MSCs, DSS + P5 3D UC-MSCs, DSS + P15 2D UC-MSCs and DSS + P15 3D UC-MSCs. Mice of normal group were fed with purified water only. At day 3, mice of DSS + P5 2D UC-MSCs, DSS + P5 3D UC-MSCs, DSS + P15 2D UC-MSCs and DSS + P15 3D UC-MSCs groups were intravenously administrated with P5 and P15 2D or 3D UC-MSCs (1×10^6 cells/ dose) respectively. Mice in normal and DSS groups were administrated with equal volume of PBS. The body weights were recorded every day. Disease activity index (DAI) calculated according to changes of body weight, diarrhea and hematochezia as previously described [23]. Four days after UC-MSCs injection, colons were entirely resected for length measurement and pathological analysis. For pathological analysis, the colon segments were fixed with 4% paraformaldehyde, embedded in paraffin and subjected to H&E staining. The conditions of inflammation and edema of colons were evaluated under a light and polarized microscopy.

2.13 Experimental T1DM and Treatment by UC-MSCs

T1DM has been induced by a single intraperitoneal injection of streptozotocin (STZ, 50 mg/kg, MP Biomedicals, USA, 02100557-CF) in female C57/BL6J mice (8 weeks old) for 5 days. The blood glucose was measured on the 8th and 11th day. The experimental T1DM mice are those the levels of blood glucose were than 11.1 mmol/L. For 3 consecutive weeks, diabetic mice were divided into 6 groups and intravenously administrated with P5 and P15 2D or 3D UC-MSCs twice (day1 and day14). At the end of the experiment, the changes in glucose metabolism, C-peptide and GHb levels were evaluated. Furthermore, histological examination of pancreatic tissues was performed.

2.14 Statistical Analysis

Statistical analysis was carried out with GraphPad Prism version 7.0 software. T-test and one-way analysis of variance (ANOVA) were used for differences between two groups and more than two groups respectively. P-value < 0.05 was considered statistically significant. The data are presented here as Mean ± Standard Error of Mean (SEM).

3. Results

3.1 3D-culture Preserves the Stemness and Immunosuppression of UC-MSCs during Long-term Passaging

MSCs are promising candidates for disease treatment and tissue regeneration. However, the stemness and immunosuppression of UC-MSCs is decreased after long-term passaging (Fig. S1A-C), resulting in failure of MSCs therapy. Here, we explored the impact of 3D-culture-based strategy on the preserve of stemness of MSCs. UC-MSCs were cultured to P3 on TCP, then were cultured by 2D and 3D method respectively. UC-MSCs were continuously passaged until to P15 (Fig. 1A). After P15, 3D-culture was superior to 2D method in the maintenance of UC-MSCs surface specific antigens (Fig. 1D, S2A). Proliferation assay revealed that 3D method was significantly improved colony formation of P15 UC-MSCs (Fig. 1B, C). Similarly, the 3D environment promoted the proliferation of P15 UC-MSCs (Fig. 1E).

Additionally, the P5 and P15 UC-MSCs were co-cultured with activated T cells respectively (Fig. 1F). The proliferation of T cells and ELISA assay for IL-6, IL-10 and TGF-β of the supernatant showed that immunosuppression of 3D UC-MSCs was enhanced compared with 2D UC-MSCs both on P5 (Fig. 1I) and P15 (Fig. 1J). Furthermore, flow cytometry analysis showed that 3D UC-MSCs inhibited the differentiation of Th1 and Th17 and promoted the differentiation of Th2 and Treg. The ratios of Th1/Th2 and Th17/Treg in T cells co-cultured with 3D UC-MSCs were significantly decreased (Fig. 1G, H, S2B). The results showed that 3D UC-MSCs can better maintain the balance of T cell subsets, and thus maintaining the immunity stability of the body.

3.2 3D-culture Preserves the Therapeutic Effects of Long-term Passaged UC-MSCs on Immune Disorders

We adopted experimental colitis mice model and T1DM, two widely used models of immune disorders. After DSS feeding and UC-MSCs transplantation, we recorded the data on mice, including loss of weight, diarrhea and bloody stool. Transplantation of P15 3D cultured MSCs was still showed the therapeutic effects on colitis, while transplantation of P15 2D cultured MSCs was less effective (Fig. 2A, B, D, S3A). Histological analysis confirmed that DSS feeding caused severe damage in colon mucosa. Tissue section displayed P5 2D and 3D MSCs had similar therapeutic effects. However, infusion of P15 3D cultured MSCs was more effective than 2D cultured MSCs on prevent damage in colon mucosa (Fig. 2C).

To test the therapeutic effects on immune disorders of long-term passaged UC-MSCs, we established a T1DM mice model by STZ. T1DM mice showed blood glucose levels higher than 11.1mmol/L, while the normal group was lower than 10mmol/L, regardless if the mice were fasted or re-fed. The results of continuous blood glucose tests showed that 3D-culture MSCs treatment provided better performance. The 3D cultured MSCs provided therapeutic effects till P15 while the 2D not (Fig. 2E). Reduced insulin sensitivity and decreased islet size were indicated by the results of oral glucose tolerance tests (OGTTs) (Fig. 2F) and pancreas histology (Fig. 2G). The 3D cultured MSCs were more effective on islet protection than 2D cultured MSCs both on P5 and P15. The histology showed that P15 3D cultured MSCs maintained their therapeutic effects (Fig. 2G). GHb assay can reflect the overall control of blood glucose in T1DM mice (Fig. 2I). The results showed that the 3D cultured MSCs was more effective on blood glucose control than 2D cultured MSCs. The P15 2D cultured MSCs were similar to the PBS group. In contrast, the P15 3D cultured MSCs were still effective (Fig. 2H). The C-peptide levels were proportional to serum insulin and can accurately reflect the secretion function of islet β cells. After 7 days infusion of MSCs, C-peptide levels of 3D cultured MSCs treated T1DM mice were maintained better, which did show significant differences compared to that of the 2D cultured MSCs (Fig. 2J).

3.3 3D Culture Supports Long-Term Expansion through YAP Activation

We then explored the mechanism of 3D culture to prevent stemness loss of long-term passaged UC-MSCs. The immunofluorescent analyses showed that 3D culture system significantly promoted the proliferation of UC-MSCs both on P5 and P15 (Fig. 3A, B). The staining against anti-active YAP1 revealed that YAP1 expressions in the nucleus were significantly enhanced by 3 times of P5 and 7 times of P15 respectively (Fig. 3C). Notably, 3D culture system increased the active YAP1 expression in the nucleus by 25 times through qPCR assay of P5 UC-MSCs (Fig. 3D). Western blot analysis also supported that 3D culture enhanced YAP activation (Fig. 3E).

3.4 Regulation of YAP is Effective on Immunosuppression of MSCs

To confirm whether the activation of YAP affect the therapeutic effects of the cells, we further investigated the function of YAP1 on UC-MSCs. We pretreated UC-MSCs with PGE2 to promoted YAP1 and verteporfin (VP), which is a YAP specific inhibitor to inhibit YAP1 [24, 25]. The immunofluorescent and western blot analysis showed that PGE2 treated UC-MSCs have higher level of YAP1, while VP treated UC-MSCs have lower level of YAP1 (Fig. 4A-D). Furthermore, the 2D UC-MSCs, PGE2-treated 2D UC-MSCs, 3D UC-MSCs and VP-treated 3D UC-MSCs were co-cultured with activated T cells respectively. Flow cytometry analysis showed that UC-MSCs inhibited the differentiation of Th1 and Th17 and promoted the differentiation of Th2 and Treg (Fig. 5A, B, S4A-D). This immunosuppression was enhanced after PGE2-treated and declined after VP-treated. The ratios of Th1/Th2 and Th17/Treg in T cells co-cultured with PGE2-treated UC-MSCs were significantly decreased while the VP-treated UC-MSCs increased. It is suggesting YAP activation preserved the therapeutic effects of MSCs.

3.5 Regulation of YAP is Effective on the Therapeutic Effects of MSCs on Immune Disorders

We next confirmed the function of YAP1 activation by experimental colitis and T1DM Model. The experimental colitis mice were divided into 6 groups (normal, DSS + PBS, DSS + 2D UC-MSCs, DSS + PGE-2D UC-MSCs, DSS + 3D UC-MSCs and DSS + VP-3D UC-MSCs). By comparing loss of weight (Fig. 6A), diarrhea, bloody stoolt (Fig. 6B), colon length (Fig. 6D, S5A) and histological analysis (Fig. 6C), PGE2-treated UC-MSCs were more effective on colitis than no-treated, while VP-treated UC-MSCs were less effective than no-treated. The experimental T1DM mice were also divided into 6 groups. The results of therapy showed that PGE2-treatment improved the therapeutic effects of UC-MSCs on blood glucose control (Fig. 6E, F), insulin sensitivity and islet protection (Fig. 6G-J). On the contrary, VP-treatment reduced the therapeutic effects of UC-MSCs (Fig. 6E-J). In this study, we demonstrated that PGE2-treated UC-MSCs could improve the therapeutic effects of UC-MSCs. On the contrary, VP-treatment decrease the therapeutic effects. It is suggested that YAP activation improves the therapeutic effects of UC-MSCs, while YAP inhibition decreases it.

4. Discussion

Due to their immunomodulatory property, MSCs have been increasingly used to treat a range of immunopathy [26, 27], and 3D cultured MSCs show enhanced immunomodulatory property compared with those in 2D culture [1]. However, both the regulatory mechanisms remain unclear. Meaningfully, we modulated YAP pathway both of 2D and 3D cultured UC-MSCs and validated its role in colitis and T1DM mouse models, which proved that mechanical stress played an important role in maintaining the immunomodulatory function and therapeutic potential of 2D and 3D cultured UC-MSCs, and PGE2 could be used to up-regulate YAP and improve the immunomodulatory ability of 2D cultured UC-MSCs after extensive expansion.

As a kind of adult stem cells, MSCs possess two characteristics that are distinct from other adult cells. First, they have stemness, as embodied by their self-renewal and tri-lineage differentiation into osteoblasts, chondrocytes and adipocytes. Second, MSCs own immunomodulatory property [28]. Studies have shown that although cell replacement plays an important role in MSCs therapy for specific diseases, the final therapeutic effects are mainly the results of MSCs-derived immunomodulatory ability of inhibiting the proliferation and functions of various immunocytes, including T lymphocytes, B lymphocytes, dendritic cells, macrophages, natural killer cells and neutrophils, suppressing the differentiation of naive $CD4^+$ T cells into proinflammatory Th1 and Th17 cell lineages and promoting the generation of Treg cells [3, 29, 30]. Here, the P5 UC-MSCs did exhibit both features, which were consistent with previous findings.

MSCs release cytokines into the microenvironment through autocrine and paracrine to maintain living conditions. The microenvironment, in turn, conducts variation of the environment in the whole body through changes in metabolism, secretion, immunity and functions, limiting and affecting the occurrence

and development of MSCs [31]. However, traditional 2D culture cannot mimic the in vivo architecture and microenvironment well. Therefore, 2D cultured MSCs display many characteristics of replicative senescence compared with in vivo MSCs [1, 32]. Furthermore, senescent cells secrete IL-6 and IL-8, which act in an autocrine and a paracrine way to reinforce senescence [33]. In this study, compared with P5 UC-MSCs, when P15 UC-MSCs were co-cultured with activated T cells, it showed enhanced T cell proliferation, increased IL-6 and decreased IL-10 and TGF-β, which may be the reasons for the decrescent therapeutic effects of 2D cultured UC-MSCs.

Increasing studies have explored drugs that can reverse the replicative senescence of MSCs. For example, reduced glutathione (GSH) and melatonin displayed an anti-senescent effect in MSCs and preserved stem cell functions including cell migration, stemness, and multidirectional differentiation potential through reducing reactive oxygen species (ROS) generation during long-term in vitro expansion [34]. Imperfection of 2D culture has also inspired the emergence of 3D cell culture systems. Up to now, various types of architectures and biomaterials that support 3D cell proliferation have been reported. For one instance, TableTrix™ (Cytoniche) is a commercially available microcarrier based on macroporous and elastic gelatin [35]. Hydrogels, a common material form, have also been successfully used to support 3D cell growth in vitro, such as Extracell™ (Dextran Biological System) [36]. However, existing drugs or products have mostly focused on retarding the senescence phenotype of MSCs and promoting the proliferation and differentiation in the process of long-term expansion, while the improvement of immunomodulatory ability, a hinge of boosting the therapeutic effects of MSCs, has not received much attention.

In a 3D culture system, cells can better communicate with neighboring cells, and the cell-to-cell and cell-to-matrix connections are reflected in the culture environment, which are consistent with the in vivo microenvironment [37, 38]. Moreover, 3D cultured MSCs significantly maintain elevated expression levels of stemness genes, yield high frequencies of colony-forming units and show enhanced osteogenic and adipogenic differentiation efficiency [39]. One research also indicated that the expressions of HLA-G, IDO1, PTGS2 and TGF-β1, which were closely related to immune regulation, were higher in 3D culture than those in 2D culture. Further, 3D cultured MSCs could inhibit the proliferation of activated lymphocytes more effectively [17]. Here, we compared the stemness and immunomodulatory ability between 2D and 3D UC-MSCs and found that 3D culture did preserve the stemness, T cell proliferative inhibition and the expression of anti-inflammatory cytokines such as IL-10 and TGF-β of long-passaged UC-MSCs. Moreover, we observed that 3D cultured UC-MSCs at P5 or P15 was more effective in treating T1DM and colitis mice than those in 2D culture, adding to the current knowledge of 3D cultured MSCs for the treatment of immune disorders.

Most notably, the morphology of MSCs in the 3D cultured systems markedly differ from those on 2D surfaces throughout the cultivation process [40], and the morphology of MSCs can be affected by a variety of mechanical properties, including elasticity, geometry and adhesion, which will ultimately affect the tension of the cytoskeleton [41]. It has been widely accepted that the transcriptional effector of the hippo pathway-the YAP/transcriptional coactivator with PDZ-binding motif (TAZ) acts as a sensor and

mediator of mechanical signals in response to extracellular matrix cues [42, 43] Meanwhile, YAP signaling is strongly activated during the culture of cells in the matrigel-encapsulated 3D culture system and maintains the proliferative capacity of the encapsulated cells [18]. In line with these phenomena, we found the YAP expression both of P5 and P15 UC-MSCs in 3D culture was significantly higher than those in 2D culture. Furthermore, we demonstrated that mechanical stress played a significant role in maintaining immunoregulatory function of 2D and 3D cultured UC-MSCs by modulating YAP pathway, and PGE2 could be used to up-regulate YAP and improve the immunomodulatory ability of long-passaged 2D cultured UC-MSCs, providing theoretical supports for the regulation of cellular immunity and therapeutic efficacy by adjusting mechanical stress.

5. Conclusions

Our study indicated that 3D culture extended the stemness, immunomodulatory ability and therapeutic effects of UC-MSCs by activating YAP pathway for several passages longer than 2D culture. In addition, YAP activation was convincingly demonstrated to be important to the immunomodulatory ability and therapeutic effects both of 2D and 3D cultured UC-MSCs, largely due to its capacity of shifting the mechanical stress during cell culture, so it can be up-regulated by PGE2 to improve the immunomodulatory ability of 2D cultured UC-MSCs after extensive expansion. This work found for the first time that the significance of mechanical stress in maintaining immunoregulatory function both of 2D and 3D cultured UC-MSCs, providing a new idea for improving the efficacy of MSCs-based immunotherapy.

Abbreviations

2D two-dimensional

3D three-dimensional

α-MEM medium-α

ANOVA analysis of variance

BCA bicinchoninic acid

CCK-8 cell counting kit-8

DAI disease activity index

DAPI 4',6-diamidino-2-phenylindole

DSS dextran sulfate sodium salt

ECM extracellular matrix

FBS fetal bovine serum

GADPH glyceraldehyde-3-phosphate dehydrogenase

GHb glycated hemoglobin

GSH reduced glutathione

HLA human leukocyte antigen

IDO indoleamine 2,3-dioxygenase

IFN interferon

IL interleukin

MSCs mesenchymal stem cells

OD optical density

OGTTs oral glucose tolerance tests

PBMCs peripheral blood mononuclear cells

PBS phosphate buffer saline

PGE2 prostaglandin E2

PTGS prostaglandin synthase

qPCR real-time quantitative polymerase chain reaction

ROS reactive oxygen species

SEM standard error of mean

STZ streptozotocin

T1DM type 1 diabetes mellitus

TAZ transcriptional coactivator with PDZ-binding motif

TCP tissue culture plastic

TGF transforming growth factor

Th T helper

TNF tumor necrosis factor

Treg regulatory T

UC-MSCs umbilical cord mesenchymal stem cells

VP verteporfin

YAP Yes-associated protein

Declarations

Ethics approval and consent to participate: UC-MSCs were isolated from human umbilical cords freshly obtained from women who gave birth in Xi'an No. 4 Hospital. All the donors signed informed consent to this study. The experimental procedures of human samples were approved by the Institutional Review Board for Human Subjects Research of Xi'an No. 4 Hospital. All animal experimental procedures were accordance with National Institutes of Health Guide for the Care and Use of Laboratory Animals and approved by Animal Care Committee of Xi'an Jiaotong University.

Consent for publication: Not applicable.

Availability of data and materials: The datasets used and analysed during the current study are available from the corresponding author on reasonable request.

Competing interests: The authors declare that they have no competing interest.

Funding: The National Key Research and Development Program of China (2017YFA0104900); Xi'an Fourth Hospital Incubation Fund Project (2019FZ46); The National Natural Science Foundation of China (81930025, 81870676).

Authors' contributions: FYD, NZ and LB contributed equally to the study design, manuscript preparation and data collection. JL, AQL and YFG made contributions to animal experiment, data acquisition and analysis. LHB and HN critically revised the manuscript. FZ, XRY and CHH supervised the research, oversaw the collection of results and data interpretation and critically revised the manuscript.

Acknowledgements: Not applicable.

References

1. Li J, Chen T, Huang X et al. Substrate-independent immunomodulatory characteristics of mesenchymal stem cells in three-dimensional culture. PLoS One. 2018; 13(11): 1-17.
2. Wang LT, Ting CH, Yen ML et al. Human mesenchymal stem cells (MSCs) for treatment towards immune- and inflammation-mediated diseases: review of current clinical trials. J Biomed Sci. 2016; 23(1): 76.

3. Wang Y, Chen X, Cao W, Shi Y. Plasticity of mesenchymal stem cells in immunomodulation: pathological and therapeutic implications. Nat Immunol. 2014; 15(11): 1009-1016.
4. Hu JX, Yu XL, Wang ZC et al. mesenchymal stem cells from the umbilical cord for newly-onset type 1 diabetes mellitus. Endocr J. 2013; 60(3): 347-357.
5. Yu S, Cheng Y, Zhang L et al. Treatment with adipose tissue-derived mesenchymal stem cells exerts anti-diabetic effects, improves long-term complications, and attenuates inflammation in type 2 diabetic rats. Stem Cell Res Ther. 2019; 10(1): 333.
6. Hu JX, Zhao G, Zhang LZ et al. Safety and therapeutic effect of mesenchymal stem cell infusion on moderate to severe ulcerative colitis. Exp Ther Med. 2016; 12(5): 2983-2989.
7. Li L, Liu S, Xu Y et al. Human umbilical cord-derived mesenchymal stem cells downregulate inflammatory responses by shifting the Treg/Th17 profile in experimental colitis. Pharmacology. 2013; 92(5-6): 257-264.
8. Yin Q, Xu N, Xu D et al. Comparison of senescence-related changes between three- and two-dimensional cultured adipose-derived mesenchymal stem cells. Stem Cell Res Ther. 2020; 11(1): 226.
9. Stab BR, Martinez L, Grismaldo A et al. Mitochondrial Functional Changes Characterization in Young and Senescent Human Adipose Derived MSCs. Front Aging Neurosci. 2016; 8: 299.
10. Fafián-Labora JA, Morente-López M, Arufe MC. Effect of aging on behaviour of mesenchymal stem cells. World J Stem Cells. 2019; 11(6): 337-346.
11. Macrin D, Alghadeer A, Zhao YT et al. Metabolism as an early predictor of DPSCs aging. Sci Rep. 2019; 9(1): 2195.
12. Khan H, Mafi P, Mafi R, Khan W. The effects of ageing on differentiation and characterisation of human mesenchymal stem cells. Curr Stem Cell Res Ther. 2018; 13(5): 378–383.
13. Antoni D, Burckel H, Josset E, Noel G. Three-dimensional cell culture: a breakthrough in vivo. Int J Mol Sci. 2015; 16(3): 5517-5527.
14. Chen Q, Wang Y. The application of three-dimensional cell culture in clinical medicine. Biotechnol Lett. 2020; 42(11): 2071-2082.
15. Behonick DJ, Werb Z. A bit of give and take: the relationship between the extracellular matrix and the developing chondrocyte. Mech Dev. 2003; 120(11): 1327-1336.
16. Bartosh TJ, Ylöstalo JH, Mohammadipoor A et al. Aggregation of human mesenchymal stromal cells (MSCs) into 3D spheroids enhances their antiinflammatory properties. PNAS. 2010; 107(31): 13724-13729.
17. Gong X, Sun D, Li Z, Shi Q, Li D, Ju X. Three-Dimensional Culture of Umbilical Cord Mesenchymal Stem Cells Effectively Promotes Platelet Recovery in Immune Thrombocytopenia. Biol Pharm Bull. 2020; 43(7): 1052-1060.
18. Xia MY, Chen Y, He YZ, Li HW, Li WY. Activation of the RhoA-YAP-β-catenin signaling axis promotes the expansion of inner ear progenitor cells in 3D culture. Stem Cells. 2020; 38: 860-874.

19. Bomo J, Ezan F, Tiaho F et al. Increasing 3D Matrix Rigidity Strengthens Proliferation and Spheroid Development of Human Liver Cells in a Constant Growth Factor Environment. J Cell Biochem. 2016; 117(3): 708-720.
20. Komatsu N, Kajiya M, Motoike S et al. Type I collagen deposition via osteoinduction ameliorates YAP/TAZ activity in 3D floating culture clumps of mesenchymal stem cell/extracellular matrix complexes. Stem Cell Res Ther. 2018; 9(1): 342.
21. Liu Y, Li J, Yao B et al. The stiffness of hydrogel-based bioink impacts mesenchymal stem cells differentiation toward sweat glands in 3D-bioprinted matrix. Mater Sci Eng C. 2021; 118: 111387.
22. Zhang Q, Li Q, Zhu J et al. Comparison of therapeutic effects of different mesenchymal stem cells on rheumatoid arthritis in mice. PeerJ. 2019; 7: 1-17.
23. Pouya S, Heidari M, Baghaei K et al. Study the effects of mesenchymal stem cell conditioned medium injection in mouse model of acute colitis. Int Immunopharmacol. 2018; 54: 86-94.
24. Kim HB, Kim M, Park YS et al. Prostaglandin E2 Activates YAP and a Positive-Signaling Loop to Promote Colon Regeneration After Colitis but Also Carcinogenesis in Mice. Gastroenterology. 2017; 152(3): 616-630.
25. Dong L, Lin F, Wu W, Liu Y, Huang W. Verteporfin inhibits YAP-induced bladder cancer cell growth and invasion via Hippo signaling pathway. Int J Med Sci. 2018; 15(6): 645-652.
26. Bouffi C, Bony C, Courties G, Jorgensen C, Noel D. IL-6-dependent PGE2 secretion by mesenchymal stem cells inhibits local inflammation in experimental arthritis. PLoS One. 2010; 5(12): e14247.
27. Rafei M, Campeau PM, Aguilar-Mahecha A et al. Mesenchymal stromal cells ameliorate experimental autoimmune encephalomyelitis by inhibiting CD4 Th17 T cells in a CC chemokine ligand 2-dependent manner. J Immunol. 2009; 182(10): 5994-6002.
28. Pittenger MF, Mackay AM, Beck SC et al. Multilineage potential of adult human mesenchymal stem cells. Science. 1999; 284: 143–147.
29. Regulski MJ. Mesenchymal Stem Cells: "Guardians of Inflammation". Wounds. 2017; 29(1): 20-27.
30. Yang M, Lin J, Tang J et al. Decreased immunomodulatory and secretory capability of aging human umbilical cord mesenchymal stem cells in vitro. Biochem Biophys Res Commun. 2020; 525(3): 633-638.
31. Mantovani A, Romero PP, Palucka AK, Marincola FM. Tumour immunity: effector response to tumour and role of the microenvironment. The Lancet. 2008; 371(9614): 771-783.
32. Kretlow JD, Jin YQ, Liu W et al. Donor age and cell passage affects differentiation potential of murine bone marrow-derived stem cells. BMC Cell Biol. 2008; 9(60): 1-13.
33. Lasry A, Ben-Neriah Y, . Senescence-associated inflammatory responses: aging and cancer perspectives. Trends Immunol. 2015; 36(4): 217-228.
34. Liao NS, Shi YJ, Zhang CL et al. Antioxidants inhibit cell senescence and preserve stemness of adipose tissue-derived stem cells by reducing ROS generation during long-term in vitro expansion. Stem Cell Res Ther. 2019; 10(1).

35. Yan XJ, Zhang K, Yang YP et al. Dispersible and Dissolvable Porous Microcarrier Tablets Enable Efficient Large-Scale Human Mesenchymal Stem Cell Expansion. Tissue Eng Part C Methods. 2020; 26(5): 263-275.
36. Maltman DJ, Przyborski SA. Developments in three-dimensional cell culture technology aimed at improving the accuracy of in vitro analyses. Biochem Soc Trans. 2010; 38(4): 1072-1075.
37. Cesarz Z, Tamama K. Spheroid Culture of Mesenchymal Stem Cells. Stem Cells Int. 2015; 2016: 1-11.
38. Muellerklieser W. Three-dimensional cell cultures: from molecular mechanisms to clinical applications. Am J Physiol. 1997; 273(1): 1109-1123.
39. Han S, Zhao Y, Xiao Z et al. The three-dimensional collagen scaffold improves the stemness of rat bone marrow mesenchymal stem cells. J Genet Genomics. 2012; 39(12): 633-641.
40. Walpita D, Hay E. Studying actin-dependent processes in tissue culture. Nat Rev Mol Cell Biol. 2002; 3(2): 137-141.
41. McBeath R, Pirone DM, Nelson CM, Bhadriraju K, Chen CS. Cell Shape, Cytoskeletal Tension, and RhoA Regulate Stem Cell Lineage Commitment. Dev Cell. 2004; 6(4): 483-495.
42. Ma SH, Meng ZP, Chen R, Guan KL. The Hippo Pathway: Biology and Pathophysiology. Annu Rev Biochem. 2019; 88(1): 577-604.
43. Totaro A, Panciera T, Piccolo S. YAP/TAZ upstream signals and downstream responses. Nature Cell Biol. 2018; 20(8): 888-899.

Figures

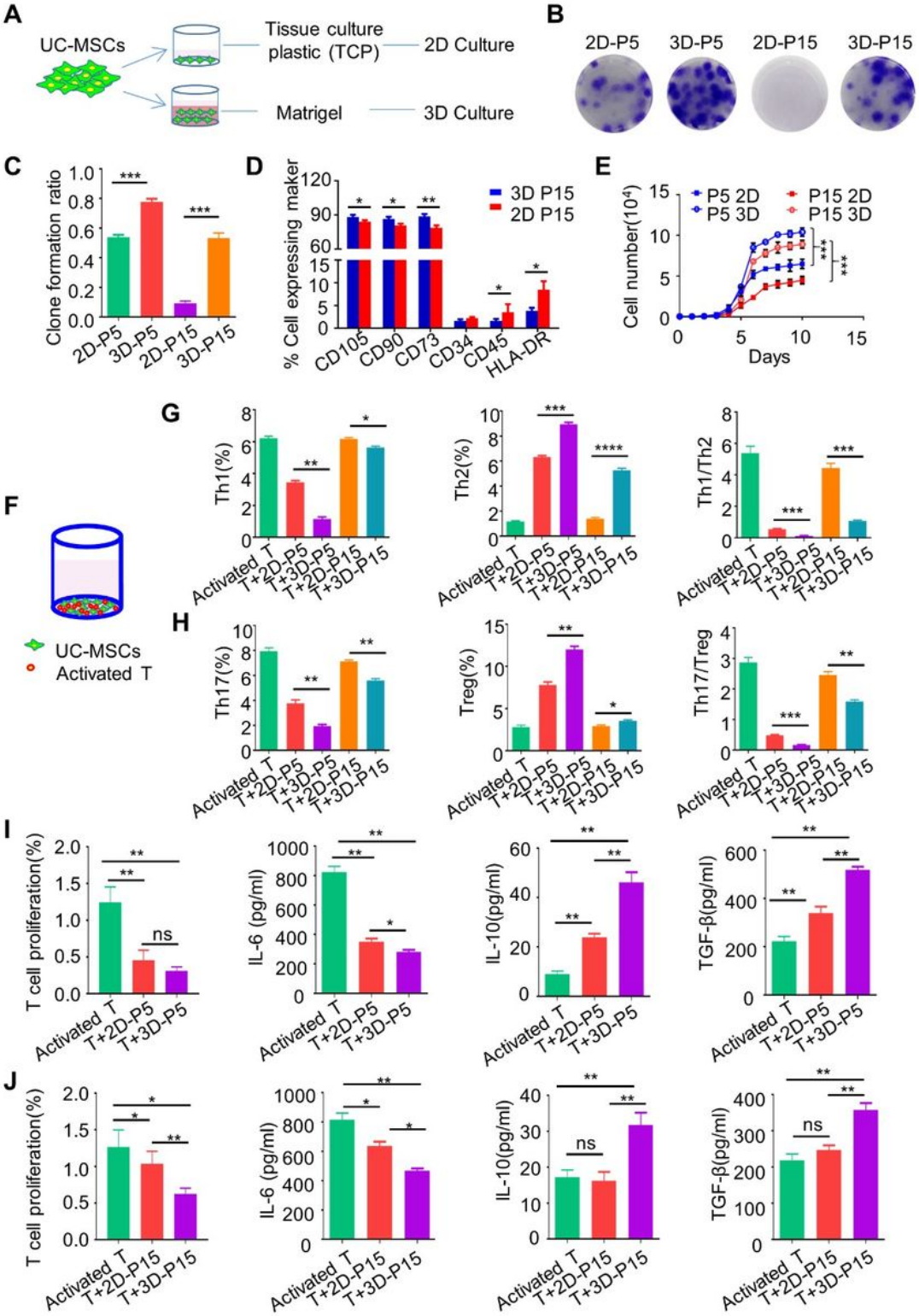

Figure 1

3D Culture Supports the Long-Term self-renew and immunoregulation of UC-MSCs. (A) The diagram of the culture methods of 2D and 3D. (B, C) CFU-F was analyzed by toluidine blue staining. (D) FACS analysis of surface markers of the P15 3D and 2D UC-MSCs. (E) Cell proliferation of the 2D and 3D UC-MSCs was analyzed with CCK-8. (F, G, H) The percentage of CD4+IFN-γ+-Th1, CD4+IL4+-Th2, CD4+IL17+-Th17 and CD4+CD25+Foxp3+-Tregs (co-cultured with the P5 or P15 UC-MSCs) were measured by FACS.

The ratios of Th1/Th2 and Th17/Treg were shown in the graphs. (I, J) Cell proliferation and cytokines in supernatant of UC-MSCs co-cultured with activated CD3+ T cells were detected by CCK-8 and ELISA. (values were shown as mean ± SD, n = 3 per group; *p < 0.05, **p < 0.01, ***p < 0.001).

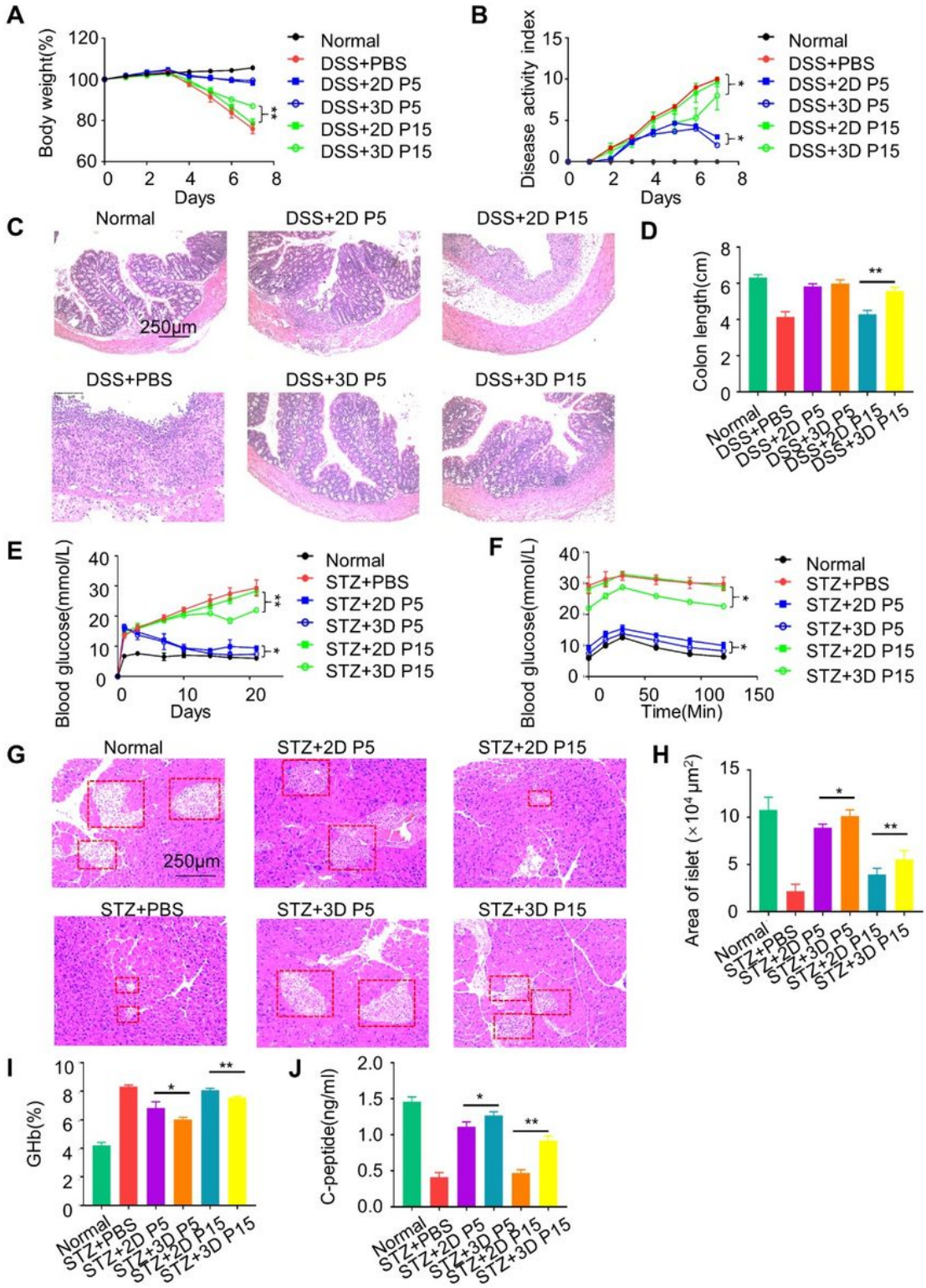

Figure 2

3D culture improves therapeutic effects of long-term passaged UC-MSCs on experimental colitis and T1DM. (A) Body weights were recorded every day for 7 days. (B) DAI was evaluated every day for 7 days.

(C) H&E staining and pathology index were performed to detect the histological changes of colon isolated at day 7. (D) Colon length was measured at day 7. (E) Blood glucose levels of each group were determined every 3 days. (F) Individual glucose tolerance was assessed by intraperitoneal injection. Fasted mice were intraperitoneally injected with 2 g of glucose/kg body weight, and blood glucose levels were determined at 0, 15,30, 60, 90, and 120 min. (G) Morphology of pancreatic islets stained with H&E (scale bar=250 μm). (H) Area of pancreatic islets in six groups sections were quantified. (I, J) GHb and C-peptide levels in serum were evaluated by ELISA at day 21 (scale bar=250 μm, values were shown as mean ± SD, n = 4 per group).

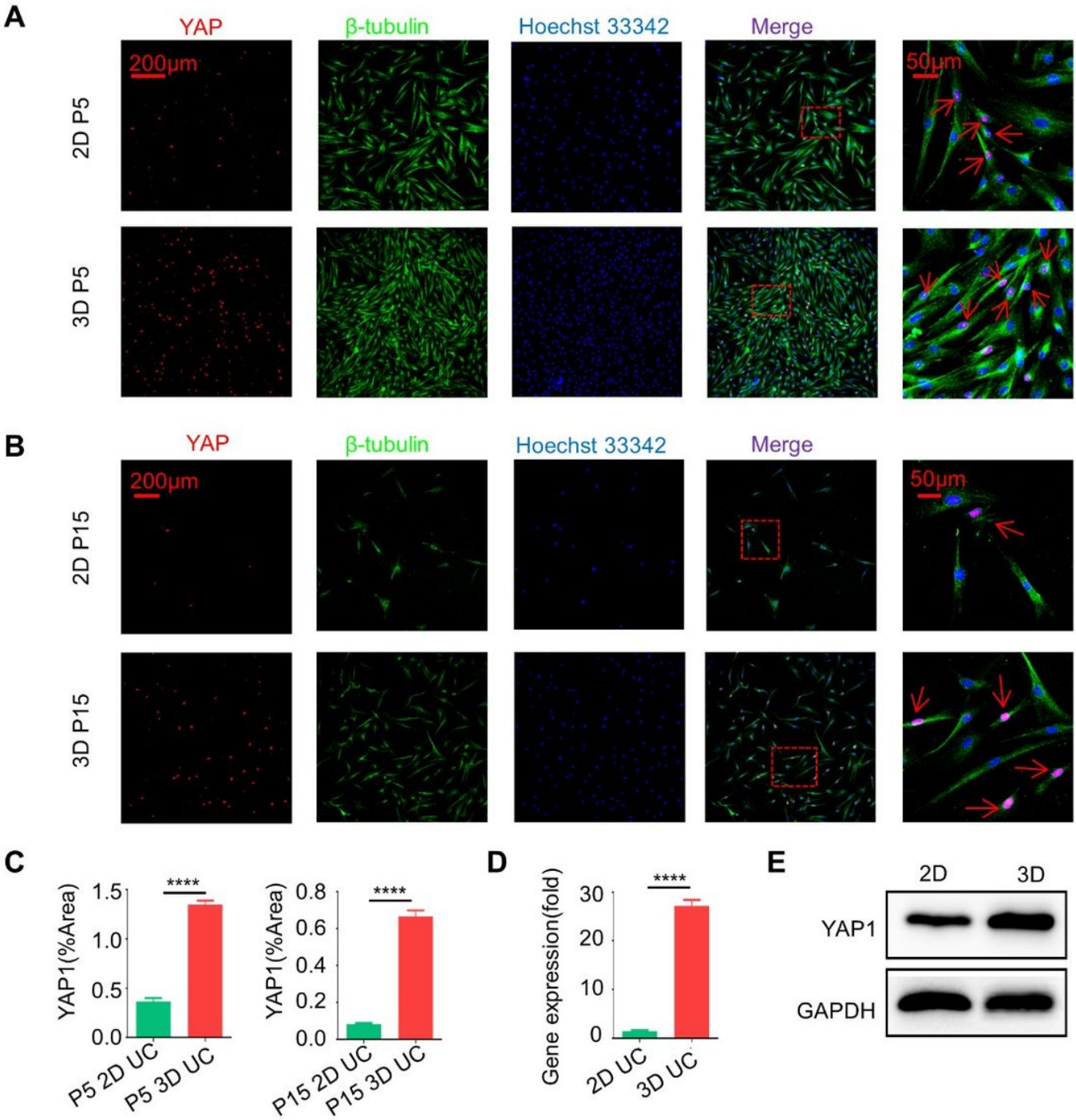

Figure 3

3D culture activated YAP1 expression in nucleus. (A-C) YAP1 staining was analyzed by immunofluorescence. (D) YAP1 levels of UC-MSCs were quantified by qPCR. (E) YAP1 of UC-MSCs was analyzed by western blot (values were shown as mean ± SD, n = 3 per group).

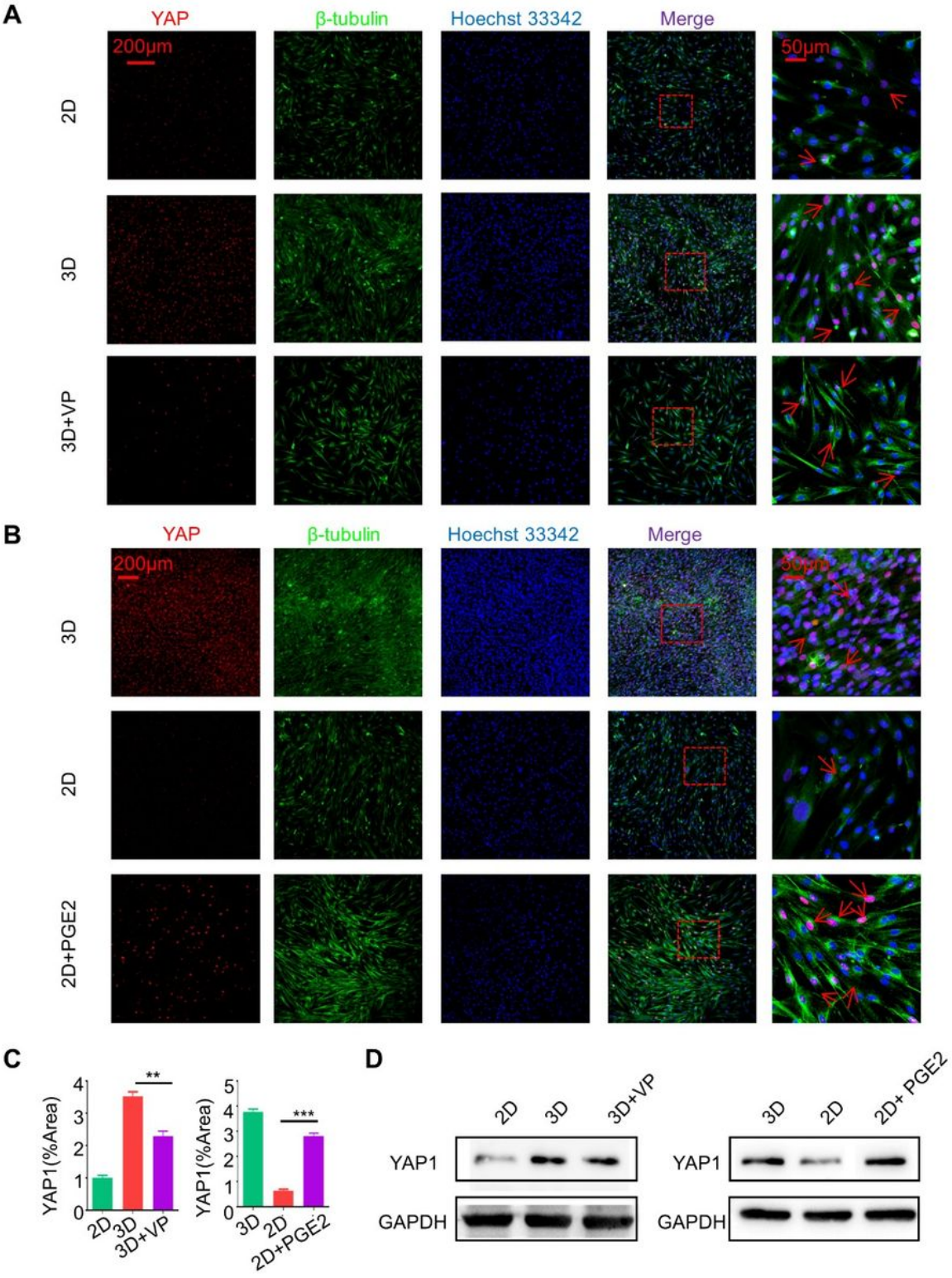

Figure 4

VP inhibited YAP1 expression in nucleus, while PGE2 promoting it. VP (10 μM) or PGE2 (10 μM) was added in the complete medium as YAP1 inhibitor and promoter for 48h. (A-C) YAP1 staining was

analyzed by immunofluorescence. (D) YAP1 of UC-MSCs was analyzed by western blot (values were shown as mean ± SD, n = 3 per group).

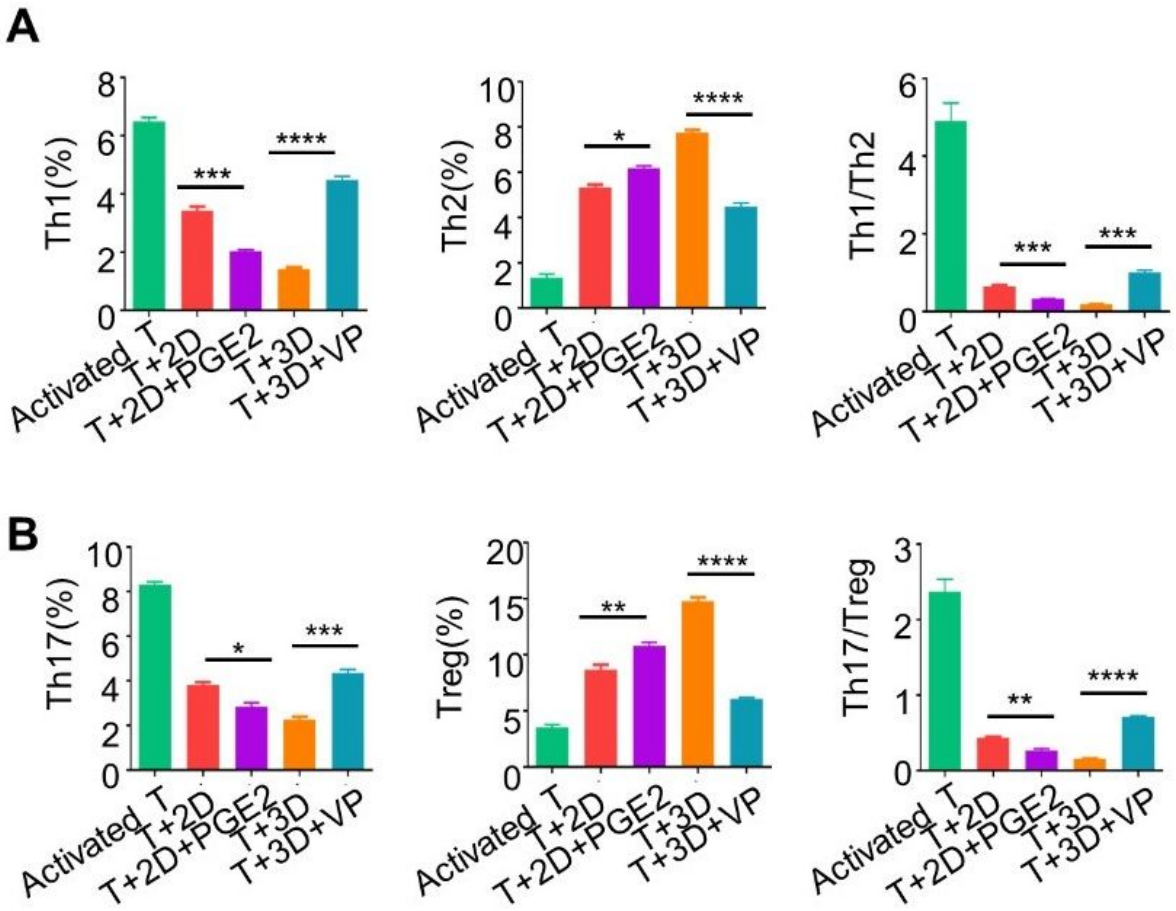

Figure 5

The relationship between immunoregulation and YAP1. (A-B) The percentage of CD4+IFN-γ+-Th1, CD4+IL4+-Th2, CD4+IL17+-Th17 and CD4+CD25+Foxp3+-Tregs (co-cultured with the P5 or P15 UC-MSCs) were measured by FACS. The ratios of Th1/Th2 and Th17/Treg were shown in the graphs (values were shown as mean ± SD, n = 3 per group).

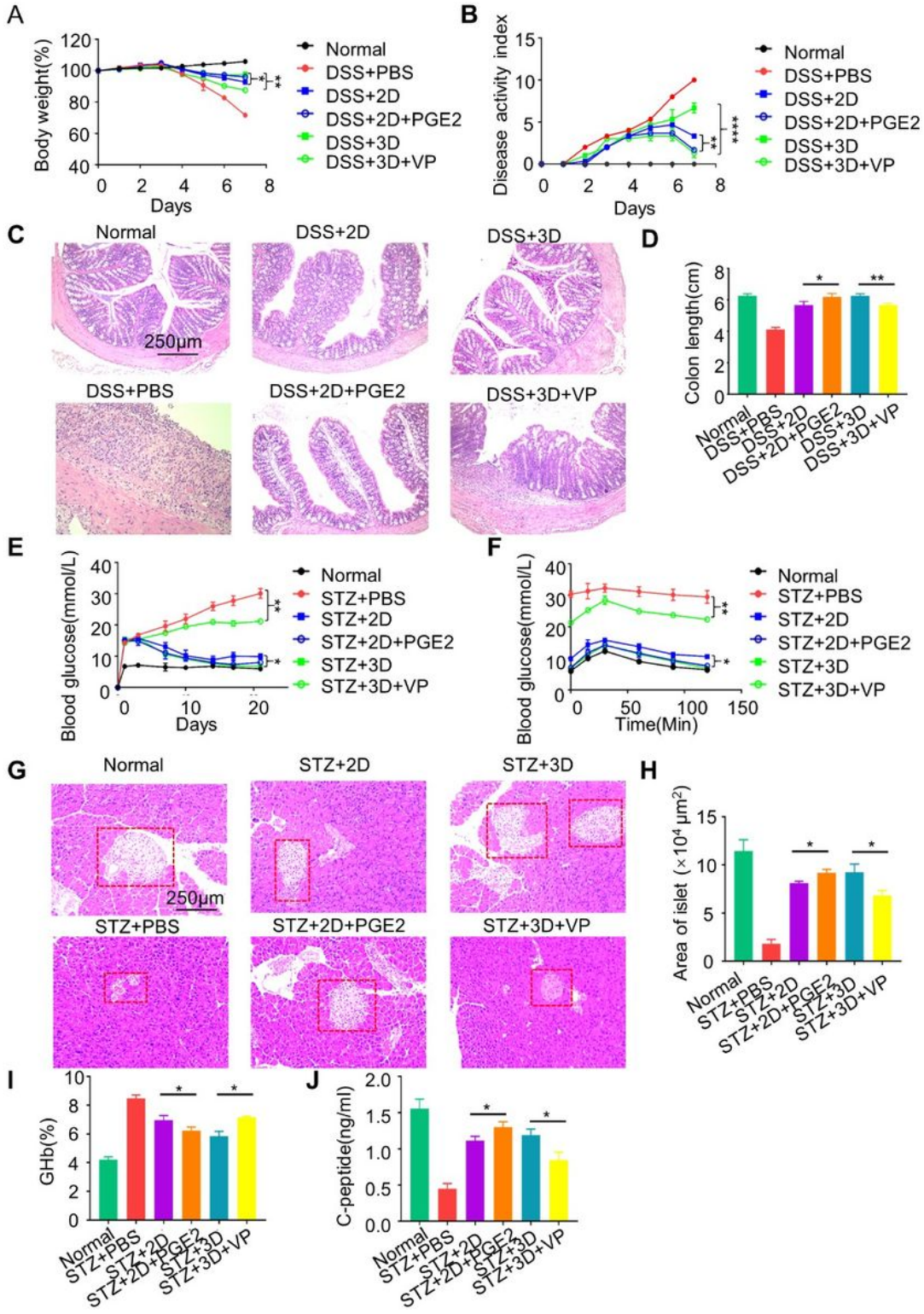

Figure 6

YAP1 influences therapeutic effects of long-term passaged UC-MSCs on experimental colitis and T1DM. (A) Body weights were recorded every day for 7 days. (B) DAI was evaluated every day for 7 days. (C) H&E staining and pathology index were performed to detect the histological changes of colon isolated at day 7. (D) Colon length was measured at day 7. (E) Blood glucose levels of each group were determined every 3 days. (F) Individual glucose tolerance was assessed by intraperitoneal injection. Fasted mice were

intraperitoneally injected with 2g of glucose/kg body weight, and blood glucose levels were determined at 0, 15,30, 60, 90, and 120 min. (G) Morphology of pancreatic islets stained with H&E (scale bar=250 μm). (H) Area of pancreatic islets in six groups sections were quantified. (I-J) GHb and C-peptide levels in serum were evaluated by ELISA at day 21 (scale bar=250 μm, values were shown as mean ± SD, n = 4 per group).

Supplementary Files

This is a list of supplementary files associated with this preprint. Click to download.

- SupplementaryData.docx
- Fig.S1.tif
- Fig.S2.tif
- Fig.S3.tif
- Fig.S4.tif
- Fig.S5.tif